Numerical and experimental investigation of the effect of bypass mass flow due to small gaps in a transonic channel flow

M. Giglmaier[1], J. F. Quaatz[1], T. Gawehn[2], A. Gülhan[2], and N. A. Adams[1]

1 Introduction

Within the joint project PAK 75 (Deutsche Forschungsgesellschaft DFG), a novel process for the production of gas phase synthesized particles is developed. The key features of the process are shock induced precursor combustion, homogeneous particle growth at constant thermodynamic conditions and gas dynamic nozzle quenching within a double choked Laval nozzle system (fig. 1) [1] [2].

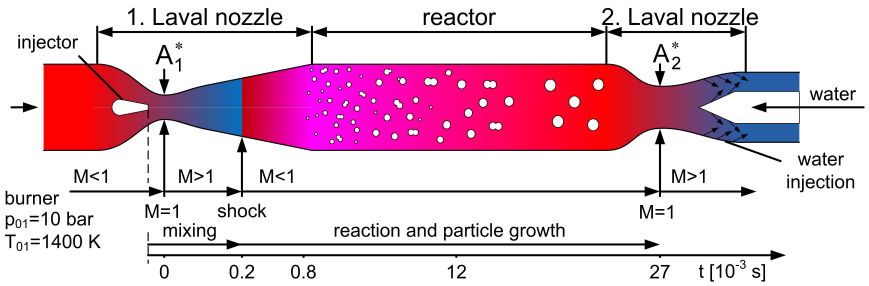

Fig. 1 Schematic of the new process of gasdynamically induced particle production

In order to guarantee a homogeneous mixture of the precursor with the carrier gas, a certain mixing length is needed. For this purpose, a low static temperature is necessary to suppress a pre-reaction of the precursor. This is achieved by accelerating the flow to supersonic speed. The required mixing length results in the development of the boundary layers that reach a maximum thickness of 15% of the

[1] *Lehrstuhl für Aerodynamik und Strömungsmechanik, Technische Universität München Boltzmannstrasse 15, 85748 Garching, Germany*
[2] *Institute of Aerodynamics and Flow Technology, Supersonic and Hypersonic Technology Department, German Aerospace Center (DLR), Linder Höhe, 51147 Cologne, Germany*

channel height at the desired shock position. The shock boundary layer interaction within the channel leads to the formation of a series of oblique shocks and rarefaction waves, a so-called pseudo-shock system. Thereby, the heating rate across the shock system is decreased, recirculation zones are formed and inhomogeneous flow conditions downstream the shock system reduce the homogeneity of the particle growth. Previous investigations within the project already improved the understanding of the dominating effects on the shock structure [3], shock asymmetry and unsteady behaviour [4], active and passive shock stabilisation and the turbulent flow characteristics shortly downstream of the shock system [5]. Pseudo-shock systems are investigated by other groups as well, a detailed review of the topic is given by [6]. Various measurement and visualisation techniques (e.g. Schlieren visualisation, LDV, PIV, LIF) require optical access to the flow. Commonly, quartz glass windows are mounted on the side walls of the test section. However, to avoid strong stresses within the glass, these windows should not be flush mounted to the facility. Thus, small gaps of $\Delta z = O(10^{-4})\ m$ can occur between the glass side walls and the metal contour. During our previous investigations we observed that these gaps result in a small bypass mass flow. Especially at high pressure gradients (e.g. shocks and critical cross sections), this mass flow results in a significant drift of the measurements. The focus of the present study is a detailed numerical analysis of the flow within the gaps and its feedback on the transonic main flow within the slender nozzle.

2 Experimental and numerical set-up

To investigate occurrence and shape, as well as the dominating mechanisms of pseudo-shock systems for a certain range of operating conditions and nozzle geometries, a test rig with optical access is build up at the DLR in Cologne.

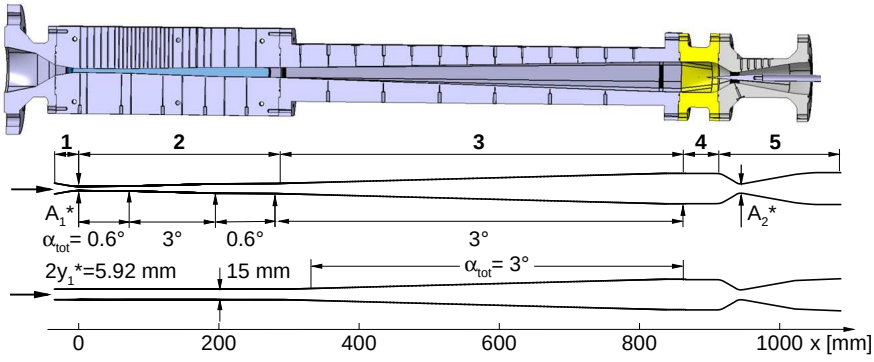

Fig. 2 Geometry of the test rig in Cologne

Similar to the previously described particle reactor, the test rig consists of a double choked Laval nozzle system (fig. 2). The primary nozzle (①, ②) is equipped with parallel quartz glass side walls in order to perform Schlieren imaging. To record the wall pressure distribution, the upper and lower contour inliners are equipped with 28 pressure sensors. The flow is further decelerated in the double divergent reactor part (③, ④). A slender movable cone within the second Laval nozzle (⑤) defines the area of the second critical cross section. For constant adiabatic mass flow, the ratio of the critical cross sections A_1^*/A_2^* is proportional to the inverse ratio of the stagnation pressure. The reduction of the stagnation pressure is caused by shock-losses and by friction. However, shock-losses can be reduced by decreasing the area of the second critical cross section. As a result, the pseudo-shock system moves upstream and re-establishes at a lower pre-shock Mach number. The influence of different nozzle shapes is investigated by two interchangeable contour inliners (fig. 3 ⓐ) within the first Laval nozzle. The gap flow is analysed for three experimental set-ups. Reference data is obtained with approximately zero gap width by using flush mounted metal side walls. Two gap sizes of 0.1 mm and 0.2 mm are investigated with quartz glass side walls mounted on both sides of the nozzle (fig. 3 ⓑ).

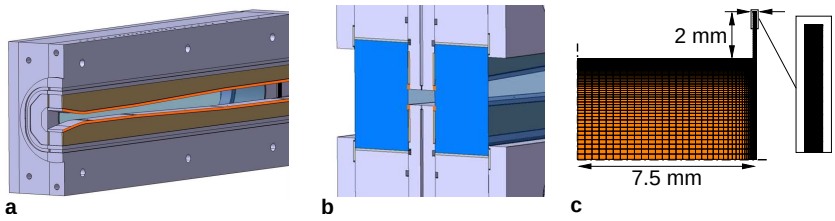

Fig. 3 a) Primary nozzle with contour inliners b) cut view through x=0 c) mesh at x=0

For the computation of the flow, the commercial pressure-based solver Ansys CFX is used. The governing equations are the 3-D time dependent Favre-averaged Navier-Stokes equations for compressible flow. By applying an explicit algebraic Reynolds stress turbulence model (EARSM) the occurrence of secondary flow, such as corner vortices in the square cross section of the reactor, is resolved. The computational effort is significantly reduced by assuming symmetry boundary conditions in order to model only one quarter of the flow field. Furthermore, the second Laval nozzle is not considered but a suitable boundary condition is used instead. Grid studies showed that $4.1 \cdot 10^6$ finite volumes (hexahedrons) provide sufficient resolution to resolve even delicate 3-D flow details arising within the channel with zero gap width. The boundary layers are resolved by at least 20 finite volumes in wall-normal direction, resulting in a dimensionless wall distance of $y^+ \leq 1$. For the computation of the gap flow, two additional grids are employed. The cross sections of the gaps along the primary nozzle (fig. 2, ① and ②) are 2 mm x 0.1 mm and 2 mm x 0.2 mm. The 0.1 mm gap is discretised with $1.7 \cdot 10^5$ additional finite volumes, the 0.2 mm

gap with additional $2.9 \cdot 10^6$ finite volumes. A planar cut of the mesh at the critical cross section is shown in fig. 3 ⓒ.

3 Experimental and numerical results

In the present study, a numerical analysis of the main effects of the gap flow is performed by investigating one characteristic operating point in detail.

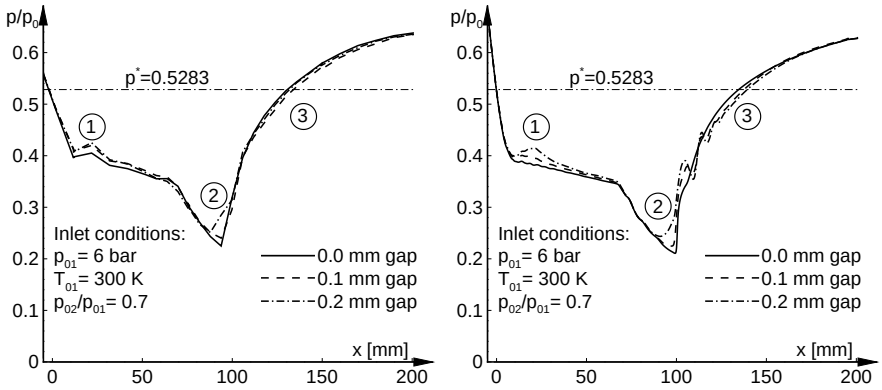

Fig. 4 Experimental (left) and numerical (right) pressure distribution along the upper nozzle wall

Figure 4 shows the experimental (left) and numerical (right) dimensionless pressure distributions along the upper wall of the primary nozzle. The critical cross section is located at $x = 0$ *mm*, the inlet conditions are $p_{01} = 6$ *bar*, $T_{01} = 300$ *K*, and a total pressure ratio of $p_{01}/p_{02} = 0.70$ is applied. Discrete measurement points are connected by line segments. The solid line represents the pressure distribution for the flow without gaps, the dashed line and the dash-dotted line indicate the pressure distributions corresponding to a gap width of 0.1 mm and 0.2 mm. The experiment shows three reproducible differences between the flow with approximately zero gap and the flows with gaps:

① The pressure directly downstream of the critical cross section increases due to the gap flow and shows a local peak at $x = 22$ *mm*.

② The pressure significantly increases ahead of the pseudo-shock system.

③ The pressure in the region of the pseudo-shock system in the case of the gap flow is slightly decreased.

One difference between the numerical results and the measurements is that the simulation without gap does not produce a local pressure peak at $x = 22$ *mm*. Since the overall tendency is clearly reproduced as soon as the gap flow is taken into account we assume that even for this configuration the experiment was not perfectly sealed. An obvious reason for the occurrence of the pressure peak can be found by

investigating the flow through the gap. Figure 5 shows the Mach number distribution together with representative streamlines on a cut plane through the middle of the gap. Since the maximum mass flow density is reached at $M = 1$, the flow is forced to enter the gap in the subsonic region slightly upstream of the critical cross section. It re-enters into the shear flow of the supersonic part downstream of the critical cross section, where mass addition leads to a deceleration of the flow and to an increase of the pressure. This mechanism is comparable to heat addition or to a reduction of the cross section in supersonic flows.

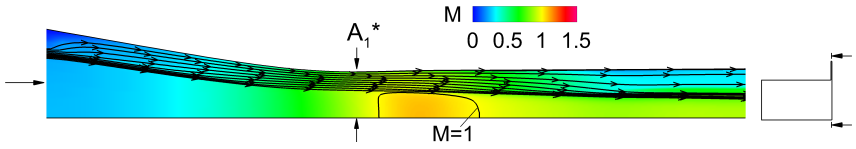

Fig. 5 Mach number distribution at a slice through the gap. Streamlines indicate the flow direction.

A significant impact of the bypass flow on the main flow can be seen by investigating the structure of the pseudo-shock system. Figure 6a) shows a simulation of the flow without gaps. The yellow iso-surface of Mach number $M = 1$ shows the supersonic flow while recirculation zones are indicated in blue (iso-surface $u = -0.01\ m/s$). One observes oblique shocks originating from all side walls at the same x-position. Recirculation zones shift the pseudo-shock system towards the centre of the channel. Figure 6b) shows the influence of the gap flow onto the shock system. In this case, the high positive pressure gradient across the shock leads to a massive reverse flow through the gaps. Therefore, the first oblique shocks are induced by a predominant corner separation and the entire pseudo-shock system is deformed. In particular, these shocks are responsible for the pre-compression observed at position ②.

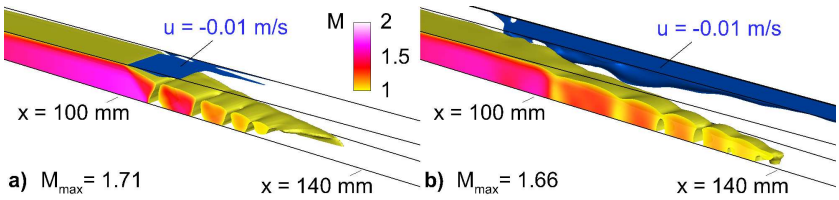

Fig. 6 Comparison of the shock system without and with gap, the yellow iso-surface with M=1 covers the supersonic flow, the blue iso-surface with u=-0.01 m/s covers the recirculation zones

This effect becomes more obvious by comparing the flow at different x-positions. The left slice in fig. 7 depicts the Mach number distribution at $x = 90\ mm$. The bypass mass flow from the gap re-enters the main flow and causes an oblique shock that can be seen at the second slice with $x = 92\ mm$. In contrast, the third slice with the same x-position for the flow without gap shows a homogeneous core flow.

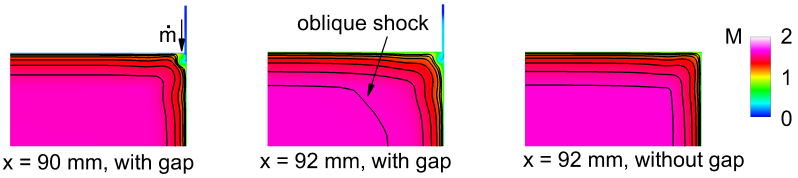

Fig. 7 Mach number distribution at different x-positions for the flow with and without gap

Another effect of the bypass flow is that the supersonic part of the shock system remains much closer to the side walls due to the suppressed separation of the entire boundary layer. This explains the numerically predicted pressure oszillations between ② and ③, which can not be resolved by the measurement. Furthermore, the displacement thickness of the corner separation increases the velocity of the core flow. Consequently, the static pressure in the pseudo-shock system and the following mixing zone (position ③) is decreased.

4 Conclusions

Our numerical investigations demonstrated that small experimental uncertainties of the facility (gap width) may result in significantly altered flow physics. For a comparison of experimental and numerical results a detailed specification of all possible uncertainties seems inevitable in case of sensitive transonic flows. Heat deformation, potential gaps and surface roughness are the predominant effects.

References

1. A. Grzona, et al.: Gas-Phase Synthesis of Non-Agglomerated Nanoparticles by Fast Gasdynamic Heating and Cooling. Shock Waves **11**, 4 (2009)
2. M. Giglmaier, N.S. Al-Hasan and N.A. Adams: 3-D Simulation of the Production of Gas-phase synthesized Non-aggregated Spherical Nano-particles in Continuous Gasdynamic Flow Particle-Laden Flows. In: *7th International Conference on Multiphase Flow - ICMF 2010 Proceedings*, VID00264, (International Conference on Multiphase Flow, 2010)
3. T. Gawehn, A. Gülhan, N.S. Al-Hasan and G.H. Schnerr: Experimental and Numerical Analysis of the Structure of Pseudo-Shock Systems in Laval Nozzles with Parallel Side Walls. Shock Waves **20**, 4 (2010)
4. T. Gawehn, A. Gülhan, M. Giglmaier, N.S. Al-Hasan and N.A. Adams: Analysis of Pseudo-Shock System Structure and Asymmetry in Laval Nozzles with Parallel Side Walls. In: *19th Interantional Shock Interaction Symposium*, Moscow (2010)
5. A. Grzona and H. Olivier: Shock train generated turbulence inside a nozzle with a small opening angle. Experiments in Fluids (2011)
6. K. Matsuo, Y. Miyazato and H.-D. Kim: Shock train and pseudo-shock phenomena in internal gas flows. In: *Progress in Aerospace Sciences, vol 35-1*, (1999)